EINDHOVEN UNIVERSITY OF TECHNOLOGY

# Area-selective deposition of Ruthenium by combining atomic layer deposition and selective etching

*Citation for published version (APA):*
Vos, M. F. J., Chopra, S. N., Verheijen, M. A., Ekerdt, J. G., Agarwal, S., Kessels, W. M. M., & Mackus, A. J. M. (2019). Area-selective deposition of Ruthenium by combining atomic layer deposition and selective etching. *Chemistry of Materials*, *31*(11), 3878-3882. https://doi.org/10.1021/acs.chemmater.9b00193

*DOI:*
10.1021/acs.chemmater.9b00193

*Document status and date:*
Published: 22/05/2019

*Document Version:*
Publisher's PDF, also known as Version of Record (includes final page, issue and volume numbers)

***Please check the document version of this publication:***

• A submitted manuscript is the version of the article upon submission and before peer-review. There can be important differences between the submitted version and the official published version of record. People interested in the research are advised to contact the author for the final version of the publication, or visit the DOI to the publisher's website.
• The final author version and the galley proof are versions of the publication after peer review.
• The final published version features the final layout of the paper including the volume, issue and page numbers.

Link to publication

*General rights*
Copyright and moral rights for the publications made accessible in the public portal are retained by the authors and/or other copyright owners and it is a condition of accessing publications that users recognise and abide by the legal requirements associated with these rights.

• Users may download and print one copy of any publication from the public portal for the purpose of private study or research.
• You may not further distribute the material or use it for any profit-making activity or commercial gain
• You may freely distribute the URL identifying the publication in the public portal.

If the publication is distributed under the terms of Article 25fa of the Dutch Copyright Act, indicated by the "Taverne" license above, please follow below link for the End User Agreement:

www.tue.nl/taverne

*Take down policy*
If you believe that this document breaches copyright please contact us at:

openaccess@tue.nl

providing details and we will investigate your claim.

Download date: 28. Aug. 2022

This is an open access article published under a Creative Commons Non-Commercial No Derivative Works (CC-BY-NC-ND) Attribution License, which permits copying and redistribution of the article, and creation of adaptations, all for non-commercial purposes.

CHEMISTRY OF MATERIALS
Communication
Cite This: Chem. Mater. 2019, 31, 3878−3882
pubs.acs.org/cm

# Area-Selective Deposition of Ruthenium by Combining Atomic Layer Deposition and Selective Etching

Martijn F. J. Vos,[†] Sonali N. Chopra,[†,‡] Marcel A. Verheijen,[†] John G. Ekerdt,[‡] Sumit Agarwal,[§] Wilhelmus M. M. Kessels,[†] and Adriaan J. M. Mackus*,[†]

[†]Department of Applied Physics, Eindhoven University of Technology, P.O. Box 513, 5600 MB Eindhoven, The Netherlands

[‡]McKetta Department of Chemical Engineering, The University of Texas at Austin, 200 East Dean Keeton Street, Stop C0400, Austin, Texas 78712, United States

[§]Department of Chemical and Biological Engineering, Colorado School of Mines, 1613 Illinois Street, Golden, Colorado 80401, United States

*Supporting Information*

Downloaded by TU EINDHOVEN at 03:40:41:432 on June 18, 2019 from https://pubs.acs.org/doi/10.1021/acs.chemmater.9b00193.

Current nanopatterning techniques used for integrated circuit fabrication typically rely on a combination of deposition, lithography, and etch steps. Due to alignment issues, nanopatterning is becoming very challenging as device dimensions approach sub-5 nm scales.[1,2] In recent years, area-selective atomic layer deposition (ALD) has emerged as an alternative, bottom-up approach to nanomanufacturing.[3,4] By limiting the deposition to specific areas, area-selective ALD enables self-aligned fabrication and can reduce the number of processing steps during device manufacturing, such as patterning and chemical mechanical polishing. Since ALD operates in a surface-reaction-controlled regime with sequential precursor and co-reactant exposures, separated by purge steps, area-selective ALD is also characterized by growth with precise thickness control and high conformality.[5,6]

Currently, one of the main challenges for industrial application of area-selective ALD is obtaining a sufficiently high selectivity.[7] The selectivity is generally limited to a few tens of ALD cycles due to eventual nucleation on the area where no deposition is desired ("non-growth area"). Cleaning based on etching has previously been implemented in industrial selective epitaxy processes,[8] which serves as inspiration here for exploring novel combinations of area-selective ALD and selective etching. For example, during the selective epitaxial growth of Si by chemical vapor deposition (CVD), an etchant gas, typically HCl, is added to the CVD gas mixture to remove unwanted nucleation on $SiO_2$ or $Si_3N_4$ nongrowth areas.[9,10] Due to the cyclewise nature of ALD, it is especially valuable to develop deposition processes that involve an *intermittent* correction or cleaning step to increase the growth selectivity.

Area-selective ALD of metal-on-metal is of interest for applications in metal interconnects in semiconductor devices. In particular, ALD of Ru is significant, since Ru (bulk resistivity of 7.1 $\mu\Omega$ cm) is considered either as a Cu diffusion barrier or as a replacement for Cu lines.[11−15] Furthermore, Ru is used as an electrode in dynamic random access memory, a gate metal in transistors, and a seed layer for electroplating.[16−21] Area-selective ALD of Ru on metal seed layers can simplify device processing for these applications. Several processes for area-selective ALD of Ru already exist and depend on inherent selectivity, area activation, or area deactivation.[22−26] Here, we demonstrate a method for area-selective ALD of Ru on Pt or Ru (metal-on-metal) with $SiO_2$ as the nongrowth area, which exploits the inherent selectivity between the two different substrate materials.

Our approach to achieve area-selective ALD with high selectivity is based on deposition and cleaning and consists of periodic selective etch steps integrated into an ALD process as illustrated in Figure 1. The resulting supercycle of ALD and etch steps offers a promising opportunity to improve the growth selectivity of ALD processes. An essential requirement for this approach is that there should be an initial difference in nucleation behavior on the different substrate areas or materials.[27] After a certain number of cycles, nuclei start to form on the nongrowth area, and the addition of etch steps can lead to removal of these nuclei. Typically, some material is also removed on the growth area, where deposition is actually desired. However, as long as substantially more material is deposited than etched on the growth area per supercycle, this approach can provide a sufficiently high net growth rate, while improving the overall growth selectivity. By repeating such a

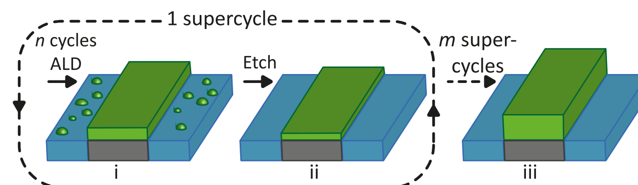


**Figure 1.** Schematic illustration of the concept of combining ALD with periodic etching to achieve area-selective deposition with a high selectivity. (i) When using an ALD process with an (insufficient) inherent selectivity, ALD leads to film growth on the growth area (gray, e.g., Pt, Ru), and island formation on the nongrowth area (blue, e.g., $SiO_2$). (ii) Inclusion of etch steps in a supercycle recipe results in removal of the unwanted deposition on the nongrowth area. (iii) By repeating the supercycle, a film with the desired thickness can be obtained selectively on the growth area.

Received: January 15, 2019
Revised: May 20, 2019
Published: May 22, 2019

supercycle of ALD and etching as many times as required, the desired thickness can be obtained on the growth area.

It is important that the following two requirements are met when combining ALD with etching to improve the selectivity of the deposition process: (i) growth-area selectivity, which refers to an initial difference in nucleation behavior (in terms of nucleation delay or growth per cycle) between the growth and nongrowth areas, and (ii) etch selectivity, where only the deposited material is etched, with almost no etching of the substrate material or other materials that are present. Several additional aspects are desirable and can lead to a more ideal area-selective ALD process. First, to retain the merits of ALD, the etching process is preferred to be self-limiting and isotropic. In the case of plasma etching, this means that the ion contribution should be insignificant. The conformal nature of ALD on 3D structures is especially preserved by combining ALD with isotropic atomic layer etching (ALE).[28] Second, the etch step should have a negligible effect on the neighboring materials and underlying substrate, for instance, in terms of roughening or incorporation of impurities. Furthermore, possible impurities should be easily removed, or at least not inhibit growth on the growth area in the subsequent ALD cycles. Note that having inhibiting species on the non-growth area can actually be beneficial for the selectivity.[27] Third, the ALD and etch processes should be compatible, meaning that they can be performed at similar conditions, such as temperature and pressure. Fourth, ideally the etch rate of the nuclei or islands on the non-growth area is higher than the etch rate of the material on the growth area, such that a high net growth rate on the growth area is obtained. In addition to considering these aspects, both the repetition frequency and the duration of the etch step should be optimized, in order to obtain the highest net growth rate.

Recently, Vallat et al. demonstrated a combination of ALD and selective etching to improve the overall selectivity of area-selective ALD.[27] In an $O_2$-plasma-enhanced ALD process for $Ta_2O_5$ that shows an inherent growth selectivity for a TiN surface over Si or $SiO_2$, $NF_3$ etching gas was added to the $O_2$ plasma step during every ninth cycle. The addition of the $NF_3$ allowed for the removal of $Ta_2O_5$ on Si and/or $SiO_2$ nongrowth areas such that the area-selective deposition of $Ta_2O_5$ on TiN could be achieved.[27]

All deposition and etching experiments were performed using a home-built ALD reactor with an inductively coupled plasma source operated at a radio frequency (RF) of 13.56 MHz.[29] The reactor walls and manifold lines were heated to 100 and 105 °C, respectively. After using the reactor for deposition of a different material, the chamber was first conditioned with 500 cycles of $Al_2O_3$ ALD followed by 500 cycles of thermal $RuO_x$ ALD (using a 60 s $O_2$ gas dose at 1 mbar as coreactant step). This procedure yielded reproducible Ru film growth. All substrates were cleaned after being loaded into the reactor and prior to the deposition using a 60 s $O_2$ plasma (100 W), followed by a 30 s reducing $H_2$ gas treatment. Small coupons of single-side polished Si wafers with thermally grown $SiO_2$ of ~430−450 nm and ALD-grown Pt or Ru on $SiO_2$/Si were used as $SiO_2$, Pt, and Ru substrates. In addition, a sample consisting of Pt lines on top of ~450 nm thick thermally grown $SiO_2$ was used to characterize the area-selective growth through scanning electron microscopy (SEM) and energy-dispersive X-ray spectroscopy (EDX) elemental mapping. The lines of 1, 2, and 3 $\mu$m width were patterned by electron-beam lithography (EBL) using poly(methyl methacrylate) resist, which was followed by evaporation of Pt (~50 nm thick) and lift-off. See the Supporting Information, Figure S1, for a more detailed description of the procedure. In situ spectroscopic ellipsometry (SE) was performed using a J.A. Woollam, Inc., M2000U ellipsometer to monitor the deposition and etching of Ru.[30,31] SE measurements were taken after every 10 ALD cycles and after every etch cycle. Additional details on the SE modeling and other analysis techniques can be found in the Supporting Information.

Ethylbenzenecyclohexadiene Ru(0) (EBCHDRu) (Hansol Chemical, Korea) was used as the Ru precursor and was heated to 90 °C.[32] Ar was used as a carrier gas, resulting in a chamber pressure of ~18 mTorr during the precursor dose. Ru films were deposited at 150 °C using a thermal ABC-type ALD process consisting of an EBCHDRu precursor pulse (step A), an $O_2$ gas pulse (step B), and $H_2$ gas pulse (step C), with durations of 15, 15, and 5 s, respectively. The additional $H_2$ pulse in this ABC-type ALD process serves to reduce surface $RuO_x$, formed during the $O_2$ gas pulse, and enables growth of metallic Ru at temperatures < 200 °C.[33] The low deposition temperature is essential for obtaining inherent growth selectivity of Ru on Pt or Ru versus $SiO_2$. The growth per cycle (GPC) on Pt or Ru is higher than on $SiO_2$ at low temperatures, whereas there is a negligible difference in GPC at temperatures ≥200 °C (see discussion about Figure 2 below). After the precursor step the line and chamber were purged with Ar for 4 s and pumped down for 5 s, while a pump step of 10 s was included after both the $O_2$ pulse and the $H_2$ pulse. A more detailed characterization of this ALD process will be published elsewhere.

It is known that exposing Ru to $O_3$ or to an $O_2$ plasma leads to formation of volatile $RuO_4$.[34,35] Therefore, an $O_2$ plasma was used to etch the unwanted Ru nucleation occurring on $SiO_2$. This radical-assisted etching process does not etch $SiO_2$ under the conditions used in these experiments. The process enables etching with high etch selectivity, which is one of the main requirements for the ALD-etch supercycle approach. Exposing Ru to an $O_2$ plasma, however, leads to surface oxidation, and therefore an etch cycle including a $H_2$ gas exposure was used. The $O_2$ plasma etching was performed using a RF power of 100 W for 20 or 30 s, while the subsequent $H_2$ gas dose was 15 s. The $H_2$ dose was found to be sufficiently long to reduce the film to metallic Ru (see Figure S2). The $O_2$ and $H_2$ pressures were set to 0.02 and 0.2 mbar, respectively, for both the ALD and the etch cycles. The etching of Ru was quasi self-limiting, with the etch rate slowing down after 10 s of $O_2$ plasma exposure. For instance, the thickness decrease was approximately 0.9 nm for 30 s $O_2$ plasma, as compared to 1.1 nm for 60 s $O_2$ plasma. The quasi self-limiting etch behavior is believed to be caused by the formation of a surface oxide, which is more slowly etched than a metallic Ru film.[34,36] The etch process will be investigated more extensively in future work.

First, the ALD of Ru was characterized on Pt and $SiO_2$ without using etch cycles. All depositions were done at 150 °C, since the difference in GPC on Pt compared to $SiO_2$ was maximum at this temperature. As shown in the inset of Figure 2a, after 400 ALD cycles there is approximately 9 nm of Ru growth on the Pt, compared to 4 nm on $SiO_2$. This difference in growth behavior is explained by the catalytic activity of Pt. We have previously reported that the dissociative chemisorption of $O_2$ and catalytic combustion of the precursor ligands enable the area-selective ALD of Pt and $Fe_2O_3$ on Pt


DOI: 10.1021/acs.chemmater.9b00193
Chem. Mater. 2019, 31, 3878−3882

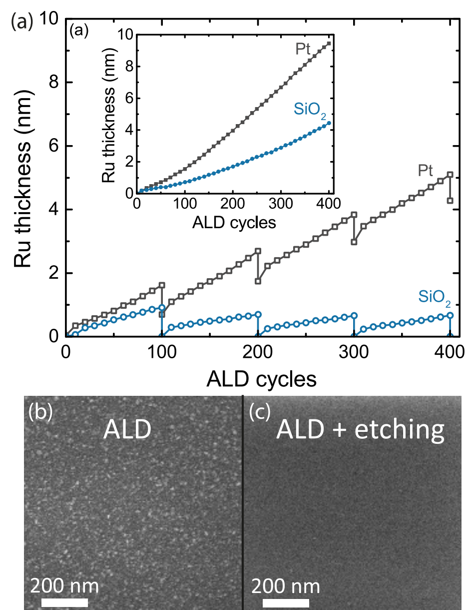


**Figure 2.** (a) Inset: Thickness as a function of ALD cycles for deposition on $SiO_2$ and Pt without etch cycles. Main figure: Ru film thickness as a function of ALD cycles for growth on $SiO_2$ and Pt with an intermittent etch cycle after every 100 ALD cycles. (b, c) Top-view SEM images after 400 ALD cycles on $SiO_2$, (b) without etch cycles, or (c) with an etch cycle after every 100 ALD cycles.

seed layers.[37,38] For the case of Ru ALD, Pt, as well as Ru, also facilitate the dissociation of $O_2$, and the formed O can subsequently lead to the combustion of the precursor ligands.[39] Since a similar pathway does not occur on the inert $SiO_2$ surface, this provides the growth selectivity of Ru on noble metals at low deposition temperatures.

To improve the selectivity of the ALD process, an etch cycle was integrated into the ALD process as illustrated in Figure 1. A supercycle recipe was performed in which one etch cycle was included after every 100 ALD cycles, using $O_2$ plasma and $H_2$ gas exposure times of 30 and 15 s, respectively. As can be seen in Figure 2a, a recipe consisting of 4 supercycles resulted in a negligible amount of Ru on $SiO_2$, while the Ru thickness on the Pt substrate was approximately 4.3 nm, as determined from SE. Approximately 1 nm of Ru is removed after each etch cycle, both on the $SiO_2$ and the Pt. However, since the GPC of Ru on Pt is higher than on $SiO_2$, the supercycle recipe results in net film deposition. A slightly enhanced growth is observed on both Pt and $SiO_2$ for the first 10 ALD cycles after each etch cycle, which is attributed to a more reactive surface due to the $O_2$ plasma exposure and subsequent $H_2$ gas dose (e.g., higher density of reactive sites). In addition, the growth rate on $SiO_2$ was found to be slightly higher during the first 100 ALD cycles as compared to each subsequent set of 100 ALD cycles, suggesting that the initial substrate has more sites on which Ru ALD can nucleate than the surface obtained after etching. The area-selective ALD of Ru on a Ru-coated substrate was also achieved using this ALD-etch supercycle, indicating that the approach is also feasible using a Ru seed layer pattern, and possibly also for other catalytic materials. The Ru deposition on $SiO_2$ was further investigated using SEM. Due to the differences in density, surface topography, and conductivity, Ru islands appear bright in the SEM images, whereas dark regions represent $SiO_2$.[40] When comparing the SEM images in Figure 2b,c, it is seen that the etch cycle using 30 s $O_2$ plasma after every 100 ALD cycles was sufficient to remove nearly all the Ru islands formed on $SiO_2$, which corroborates the results of Figure 2a.

Analysis of the nuclei visible with SEM yields a surface coverage $\theta$ on the nongrowth area of 0.0013, which corresponds to a selectivity factor $S$ of 0.997 for a Ru thickness of 4.3 nm on the Pt growth area.[41] Furthermore, XPS measurements in the region corresponding to C 1s/Ru 3d (294 eV−276 eV, see Figure S3) only revealed a small C 1s singlet peak, whereas no Ru 3d doublet peak was detected. The XPS detection limit for Ru on top of $SiO_2$ was estimated to be below 0.01 monolayer, or $1.7 \times 10^{13}$ atoms/cm$^2$.[42] Interestingly, the data demonstrates that the sensitivity for Ru nuclei detection is higher for SEM than for XPS.

After demonstrating the principle of the supercycle approach on blanket substrates, deposition was done onto a $SiO_2$ substrate with patterned Pt lines. A supercycle recipe of 800 ALD cycles was performed with an etch cycle after every 100 ALD cycles using an $O_2$ plasma time of 20 s. An etch time of 20 s was used, since this was found to be sufficiently long to obtain selectivity. The SEM image in Figure 3a shows a clean

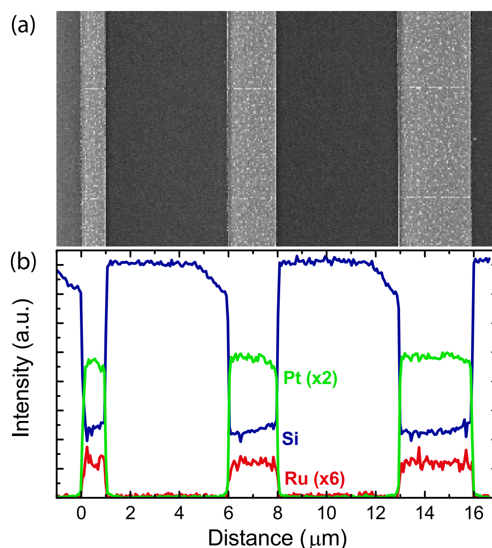


**Figure 3.** (a) SEM image and (b) corresponding EDX line scan of a patterned substrate with alternating lines of Pt (bright) and $SiO_2$ (dark) after 800 ALD cycles. The etch cycle was performed after every 100 Ru ALD cycles, using an $O_2$ plasma duration of 20 s. Note that the small white spots present on the Pt lines in (a) originate from resist residue remaining after development and before Pt evaporation. The Ru and Pt signals in (b) were rescaled for clarity.

$SiO_2$ surface in between the Pt lines, further demonstrating the selectivity of the approach. In addition, Ru was only detected by EDX on top of the Pt lines (see Figure 3b). Furthermore, the cross-sectional TEM image and EDX mapping in Figure 4a,b (of the sample as used for Figure 3) reveal that the Ru film on the evaporated Pt (~50 nm) is approximately 8 nm thick and conformally coats the Pt. The EDX mapping in Figure 4c, collected at the edge of one of the Pt lines, demonstrates that the Ru only covers the Pt and not the $SiO_2$ substrate, corroborating that a high selectivity is achieved.

The obtained material properties were investigated to further assess the potential of the ALD-etch supercycle approach. XPS measurements revealed a Ru film of high purity, and only a small O 1s peak was detected


DOI: 10.1021/acs.chemmater.9b00193
Chem. Mater. 2019, 31, 3878−3882

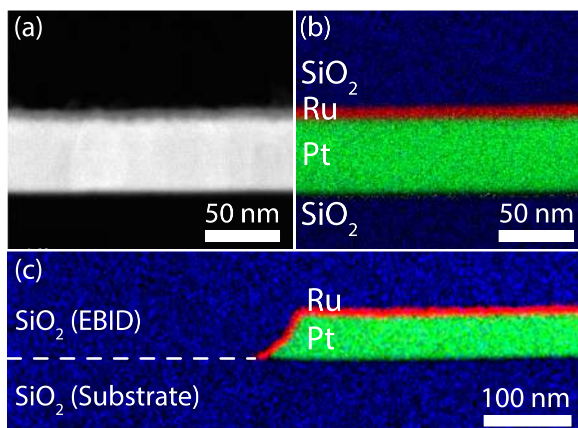


**Figure 4.** (a) Cross-sectional high-angle annular dark field scanning TEM image of a Pt line with approximately 8 nm of Ru. (b) EDX elemental mapping of the corresponding region. (c) EDX elemental mapping at the edge of a Pt line, showing the high selectivity of the Ru ALD-etch supercycle recipe. The $SiO_2$ layer at the top was deposited by electron-beam induced deposition (EBID) to protect the Pt/Ru structure during TEM-lamella preparation.

(corresponding to <5 atomic % O), which is comparable in intensity as for ALD only (see Figure S4). Furthermore, four-point-probe measurements yielded a resistivity of ~22 $\mu\Omega$ cm (after correcting for the Pt resistance) for 8 nm of Ru deposited using ALD-etch supercycles.

Comparing the growth on Pt with and without etch cycles in Figure 2a, it is clear that the GPC increases with the number of cycles when no etching is performed, while this effect seems to be suppressed by the periodic etch cycles (see also Figure S5). Note that the GPC is essentially given by the slope of the plot for the thickness versus ALD cycles. The gradual increase in GPC for the normal ALD recipe is attributed to an increase in surface roughness as the film thickness increases, which manifests as an effective increase in the surface area available for growth.[43] We speculate that this increase in GPC is suppressed by the etch cycles, as the radical-assisted $O_2$ plasma etching leads to smoothing of the Ru film. This smoothing effect can be explained by the fact that Ru regions protruding from the surface are more easily etched by the $O_2$ plasma than smooth regions of the Ru film. Smoothing of thin films, including Ru, by ALE has been reported previously, and the $O_2$ plasma etching process used in this work can be qualified as quasi-ALE.[44] To confirm this hypothesis, Ru films of ~8 nm were analyzed by AFM, yielding root-mean-square roughness values of 1.3 and 0.9 nm for films deposited without and with etch cycles, respectively. The inclusion of the etch cycles thus has the benefit of smoothing the Ru film, in addition to enhancing the selectivity.

In summary, it was demonstrated that area-selective ALD with high selectivity can be obtained by combining ALD with selective etching. Specifically, a Ru ALD process was combined with etch cycles of $O_2$ plasma and $H_2$ gas to remove unwanted growth on $SiO_2$. Approximately 8 nm of Ru was deposited on Pt patterns, while both EDX and SEM confirmed that the neighboring $SiO_2$ was clean. In addition, it was found that inclusion of the etch cycles leads to smoothing of the Ru film, as evidenced by a lower surface roughness than for ALD only. This study provides valuable insight into how area-selective ALD can be combined with selective etching to deposit materials on a surface with high selectivity, while maintaining the ALD merits of high conformality and precise thickness control. Finally, the general requirements and guidelines for ALD-etch supercycles discussed in this work can help to extend the approach to other material systems.

## ■ ASSOCIATED CONTENT

### Supporting Information

The Supporting Information is available free of charge on the ACS Publications website at DOI: 10.1021/acs.chemmater.9b00193.

Information on the process flow for the Pt pattern fabrication, additional experimental details, O 1s and Ru 3d XPS spectra collected on Pt and $SiO_2$, and Ru film thickness versus ALD cycles on Pt, with and without etch cycles (PDF)

## ■ AUTHOR INFORMATION

### Corresponding Author

*(A.J.M.M.) E-mail: a.j.m.mackus@tue.nl.

### ORCID

Martijn F. J. Vos: 0000-0002-7380-5032
John G. Ekerdt: 0000-0002-1788-5330
Wilhelmus M. M. Kessels: 0000-0002-7630-8226
Adriaan J. M. Mackus: 0000-0001-6944-9867

### Author Contributions

M.F.J.V. and S.N.C. performed the experiments and M.A.V. the TEM analysis. The manuscript was written through contributions of all authors. All authors have given approval to the final version of the manuscript.

### Notes

The authors declare no competing financial interest.

## ■ ACKNOWLEDGMENTS

The authors would like to thank C.A.A. van Helvoirt, J.J.A. Zeebregts, C.O. van Bommel, and J.J.L.M. Meulendijks for their technical assistance. R. Mahlouji, B. Barcones Campo, and D.A. Kane are acknowledged for preparation of the Pt lines on $SiO_2$, the TEM lamella, and AFM measurements, respectively. This work was financially supported by The Netherlands Organization for Scientific Research (NWO) through the Zwaartekracht program "Research Centre for Integrated Nanophotonics". In addition, the work of S.N.C. was made possible through the National Science Foundation (NSF) Graduate Research Opportunities Worldwide program and a NASCENT Whaley fellowship. Solliance and the Dutch province of Noord-Brabant are acknowledged for funding the TEM facility.

## ■ REFERENCES

(1) Schuegraf, K.; Abraham, M. C.; Brand, A.; Naik, M.; Thakur, R. Semiconductor Logic Technology Innovation to Achieve sub-10 nm Manufacturing. *IEEE J. Electron Devices Soc.* **2013**, *1*, 66−75.

(2) Thoms, S.; Macintyre, D. S.; Docherty, K. E.; Weaver, J. M. R. Alignment Verification for Electron Beam Lithography. *Microelectron. Eng.* **2014**, *123*, 9−12.

(3) Fang, M.; Ho, J. C. Area-Selective Atomic Layer Deposition: Conformal Coating, Subnanometer Thickness Control, and Smart Positioning. *ACS Nano* **2015**, *9*, 8651−8654.

(4) Mackus, A. J. M.; Bol, A. A.; Kessels, W. M. The Use of Atomic Layer Deposition in Advanced Nanopatterning. *Nanoscale* **2014**, *6*, 10941−10960.

(5) Leskelä, M.; Ritala, M. Atomic Layer Deposition (ALD): From Precursors to Thin Film Structures. *Thin Solid Films* **2002**, *409*, 138−146.
(6) George, S. M. Atomic Layer Deposition: An Overview. *Chem. Rev.* **2010**, *110*, 111−131.
(7) Mackus, A. J. M.; Merkx, M. J. M.; Kessels, W. M. M. From the Bottom-Up: Toward Area-Selective Atomic Layer Deposition with High Selectivity. *Chem. Mater.* **2019**, *31*, 2−12.
(8) Jastrzebski, L. SOI by CVD: Epitaxial Lateral Overgrowth (ELO) Process - Review. *J. Cryst. Growth* **1983**, *63*, 493−526.
(9) Rai-Choudhury, P.; Schroder, D. K. Selective Growth of Epitaxial Silicon and Gallium Arsenide. *J. Electrochem. Soc.* **1971**, *118*, 107.
(10) Goulding, M. R. The Selective Epitaxial Growth of Silicon. *Mater. Sci. Eng., B* **1993**, *17*, 47−67.
(11) Dean, J. A. *Lange's Handbook of Chemistry*, 15th ed.; McGraw-Hill: New York, 1999; Vol. 5.
(12) Henderson, L. B.; Ekerdt, J. G. Time-to-Failure Analysis of 5 Nm Amorphous Ru(P) as a Copper Diffusion Barrier. *Thin Solid Films* **2009**, *517*, 1645−1649.
(13) Arunagiri, T. N.; Zhang, Y.; Chyan, O.; El-Bouanani, M.; Kim, M. J.; Chen, K. H.; Wu, C. T.; Chen, L. C. 5 nm Ruthenium Thin Film As a Directly Plateable Copper Diffusion Barrier. *Appl. Phys. Lett.* **2005**, *86*, 083104.
(14) Tokei, Z.; Ciofi, I.; Roussel, P.; Debacker, P.; Raghavan, P.; Van Der Veen, M. H.; Jourdan, N.; Wilson, C. J.; Gonzalez, V. V.; Adelmann, C.; et al. On-Chip Interconnect Trends, Challenges and Solutions: How to Keep RC and Reliability under Control. *2016 IEEE Symp. VLSI Technol.* **2016**, 1−2.
(15) Wen, L. G.; Roussel, P.; Pedreira, O. V.; Briggs, B.; Groven, B.; Dutta, S.; Popovici, M. I.; Heylen, N.; Ciofi, I.; Vanstreels, K.; et al. Atomic Layer Deposition of Ruthenium with TiN Interface for sub-10 nm Advanced Interconnects beyond Copper. *ACS Appl. Mater. Interfaces* **2016**, *8*, 26119−26125.
(16) Kim, S. K.; Kim, W. D.; Kim, K. M.; Hwang, C. S.; Jeong, J. High Dielectric Constant $TiO_2$ Thin Films on a Ru Electrode Grown at 250 °C by Atomic-Layer Deposition. *Appl. Phys. Lett.* **2004**, *85*, 4112−4114.
(17) Kwon, O. J.; Cha, S. H.; Kim, J. J. Ruthenium Bottom Electrode Prepared by Electroplating for a High Density DRAM Capacitor. *J. Electrochem. Soc.* **2004**, *151*, C127−132.
(18) Schaekers, M.; Capon, B.; Detavernier, C.; Blasco, N. The Deposition of Ru and $RuO_2$ Films For DRAM Electrode. *ECS Trans.* **2010**, *33*, 135−144.
(19) Suh, Y.-S.; Lazar, H.; Chen, B.; Lee, J.-H.; Misra, V. Electrical Characteristics of $HfO_2$ Dielectrics with Ru Metal Gate Electrodes. *J. Electrochem. Soc.* **2005**, *152*, F138.
(20) Waechtler, T.; Ding, S. F.; Hofmann, L.; Mothes, R.; Xie, Q.; Oswald, S.; Detavernier, C.; Schulz, S. E.; Qu, X. P.; Lang, H.; et al. ALD-Grown Seed Layers for Electrochemical Copper Deposition Integrated with Different Diffusion Barrier Systems. *Microelectron. Eng.* **2011**, *88*, 684−689.
(21) Yeo, S.; Choi, S. H.; Park, J. Y.; Kim, S. H.; Cheon, T.; Lim, B. Y.; Kim, S. Atomic Layer Deposition of Ruthenium (Ru) Thin Films Using Ethylbenzen-Cyclohexadiene Ru(0) as a Seed Layer for Copper Metallization. *Thin Solid Films* **2013**, *546*, 2−8.
(22) Färm, E.; Lindroos, S.; Ritala, M.; Leskelä, M. Microcontact Printed $RuO_x$ Film as an Activation Layer for Selective-Area Atomic Layer Deposition of Ruthenium. *Chem. Mater.* **2012**, *24*, 275−278.
(23) Zyulkov, I.; Krishtab, M.; De Gendt, S.; Armini, S. Selective Ru ALD as a Catalyst for Sub-Seven-Nanometer Bottom-Up Metal Interconnects. *ACS Appl. Mater. Interfaces* **2017**, *9*, 31031−31041.
(24) Park, K. J.; Doub, J. M.; Gougousi, T.; Parsons, G. N. Microcontact Patterning of Ruthenium Gate Electrodes by Selective Area Atomic Layer Deposition. *Appl. Phys. Lett.* **2005**, *86*, 051903.
(25) Junige, M.; Löffler, M.; Geidel, M.; Albert, M.; Bartha, J. W.; Zschech, E.; Rellinghaus, B.; Dorp, W. F. V. Area-Selective Atomic Layer Deposition of Ru on Electron-Beam-Written Pt(C) Patterns versus $SiO_2$ Substratum. *Nanotechnology* **2017**, *28*, 395301.
(26) Minjauw, M. M.; Rijckaert, H.; Van Driessche, I.; Detavernier, C.; Dendooven, J. Nucleation Enhancement and Area-Selective Atomic Layer Deposition of Ruthenium Using $RuO_4$ and $H_2$ Gas. *Chem. Mater.* **2019**, *31*, 1491−1499.
(27) Vallat, R.; Gassilloud, R.; Eychenne, B.; Vallée, C. Selective Deposition of $Ta_2O_5$ by Adding Plasma Etching Super-Cycles in Plasma Enhanced Atomic Layer Deposition Steps. *J. Vac. Sci. Technol., A* **2017**, *35*, 01B104.
(28) Lee, Y.; Huffman, C.; George, S. M. Selectivity in Thermal Atomic Layer Etching Using Sequential, Self-Limiting Fluorination and Ligand-Exchange Reactions. *Chem. Mater.* **2016**, *28*, 7657−7665.
(29) Heil, S. B. S.; Langereis, E.; Roozeboom, F.; van de Sanden, M. C. M.; Kessels, W. M. M. Low-Temperature Deposition of TiN by Plasma-Assisted Atomic Layer Deposition. *J. Electrochem. Soc.* **2006**, *153*, G956.
(30) Langereis, E.; Heil, S. B. S.; Knoops, H. C. M.; Keuning, W.; van de Sanden, M. C. M.; Kessels, W. M. M. In Situ Spectroscopic Ellipsometry as a Versatile Tool for Studying Atomic Layer Deposition. *J. Phys. D: Appl. Phys.* **2009**, *42*, 073001.
(31) Leick, N.; Weber, J. W.; Mackus, A. J. M.; Weber, M. J.; van de Sanden, M. C. M.; Kessels, W. M. M. In Situ Spectroscopic Ellipsometry during Atomic Layer Deposition of Pt, Ru and Pd. *J. Phys. D: Appl. Phys.* **2016**, *49*, 269601.
(32) Hong, T. E.; Choi, S.-H.; Yeo, S.; Park, J.-Y.; Kim, S.-H.; Cheon, T.; Kim, H.; Kim, M.-K.; Kim, H. Atomic Layer Deposition of Ru Thin Films Using a Ru(0) Metallorganic Precursor and $O_2$. *ECS J. Solid State Sci. Technol.* **2013**, *2*, P47−P53.
(33) Lu, J.; Elam, J. W. Low Temperature ABC-Type Ru Atomic Layer Deposition through Consecutive Dissociative Chemisorption, Combustion, and Reduction Steps. *Chem. Mater.* **2015**, *27*, 4950−4956.
(34) Nakahara, M.; Tsunekawa, S.; Watanabe, K.; Arai, T.; Yunogami, T.; Kuroki, K. Etching Technique for Ruthenium with a High Etch Rate and High Selectivity Using Ozone Gas. *J. Vac. Sci. Technol., B: Microelectron. Process. Phenom.* **2001**, *19*, 2133.
(35) Hsu, C. C.; Coburn, J. W.; Graves, D. B. Etching of Ruthenium Coatings in $O_2$- and $Cl_2$-Containing Plasmas. *J. Vac. Sci. Technol., A* **2006**, *24*, 1−8.
(36) Saito, S.; Kuramasu, K. Plasma Etching of $RuO_2$ Thin Films. *Jpn. J. Appl. Phys.* **1992**, *31*, 135−138.
(37) Mackus, A. J. M.; Thissen, N. F. W.; Mulders, J. J. L.; Trompenaars, P. H. F.; Verheijen, M. A.; Bol, A. A.; Kessels, W. M. M. Direct-Write Atomic Layer Deposition of High-Quality Pt Nanostructures: Selective Growth Conditions and Seed Layer Requirements. *J. Phys. Chem. C* **2013**, *117*, 10788−10798.
(38) Singh, J. A.; Thissen, N. F. W.; Kim, W. H.; Johnson, H.; Kessels, W. M. M.; Bol, A. A.; Bent, S. F.; Mackus, A. J. M. Area-Selective Atomic Layer Deposition of Metal Oxides on Noble Metals through Catalytic Oxygen Activation. *Chem. Mater.* **2018**, *30*, 663−670.
(39) Leick, N.; Agarwal, S.; Mackus, A. J. M.; Potts, S. E.; Kessels, W. M. M. Catalytic Combustion Reactions During Atomic Layer Deposition of Ru Studied Using $^{18}O_2$ Isotope Labeling. *J. Phys. Chem. C* **2013**, *117*, 21320−21330.
(40) Cazaux, J. From the Physics of Secondary Electron Emission to Image Contrasts in Scanning Electron Microscopy. *J. Electron Microsc.* **2012**, *61*, 261−284.
(41) Parsons, G. N. Functional Model for Analysis of ALD Nucleation and Quantification of Area-Selective Deposition. *J. Vac. Sci. Technol., A* **2019**, *37*, 020911.
(42) Shard, A. G. Detection Limits in XPS for More than 6000 Binary Systems Using Al and Mg K$\alpha$ X-Rays. *Surf. Interface Anal.* **2014**, *46*, 175−185.
(43) Nilsen, O.; Karlsen, O. B.; Kjekshus, A.; Fjellvåg, H. Simulation of Growth Dynamics in Atomic Layer Deposition. Part III. Polycrystalline Films from Tetragonal Crystallites. *Thin Solid Films* **2007**, *515*, 4550−4558.
(44) Kanarik, K. J.; Tan, S.; Gottscho, R. A. Atomic Layer Etching: Rethinking the Art of Etch. *J. Phys. Chem. Lett.* **2018**, *9*, 4814−4821.




DOI: 10.1021/acs.chemmater.9b00193
Chem. Mater. 2019, 31, 3878−3882